

Modulation of Transient receptor potential melastatin 3 by protons through its intracellular binding sites

Md Zubayer Hossain Saad ^{1,2,#}, Liuruimin Xiang ^{1,2,#}, Yan-Shin Liao ³, Leah R. Reznikov ³,
Jianyang Du^{1,2,4,*}

¹ Department of Anatomy and Neurobiology, University of Tennessee Health Science Center, Memphis, TN 38163, USA.

² Department of Biological Sciences, University of Toledo, Toledo, OH 43606, USA.

³ Department of Physiological Sciences, University of Florida, Gainesville, FL 32610, USA.

⁴ Neuroscience Institute, University of Tennessee Health Science Center, Memphis, TN 38163, USA.

These authors contributed equally to this work

Correspondence

Jianyang Du, Tel: 901-448-3463, Email: jdu15@uthsc.edu

Running Title: Intracellular acidic pH inhibits TRPM3.

1 **Abstract**

2 Transient receptor potential melastatin 3 channel (TRPM3) is a calcium-permeable
3 nonselective cation channel that plays an important role in modulating glucose homeostasis
4 in the pancreatic beta cells. However, how TRPM3 is regulated under physiological and
5 pathological conditions is poorly understood. In this study, we found that both intracellular
6 and extracellular protons block TRPM3 through its intracellular binding sites. We
7 demonstrated that external protons indirectly block TRPM3, whereas internal protons
8 inhibit TRPM3 directly with an inhibitory pH_{50} of 6.9 ± 0.11 . We identified three titratable
9 residues, D1059, D1062, and D1073, at the inner vestibule of the channel pore that
10 contribute to pH sensitivity. The mutation of D1073Q reduces TRPM3 current intensity
11 and pH sensitivity; Replacement of Asp 1073 by Gln 1073 changes the reduction of
12 TRPM3 outward current by low external pH 5.5, from $62 \pm 3 \%$ in WT to $25 \pm 6.0 \%$ in
13 D1073Q. These results indicate that D1073 is not only essential for intracellular pH
14 sensitivity, but it is also crucial for TRPM3 channel gating. In addition, a single mutation
15 of D1059 or D1062 enhances pH sensitivity. In summary, our findings provide a novel
16 molecular determinant for pH regulation of TRPM3. The inhibition of TRPM3 by protons
17 may indicate an endogenous mechanism governing TRPM3 gating and its physiological/
18 pathological functions.

19

20 **Keywords:** TRP channels, TRPM3, protons, Pregnenolone Sulfate, Site-directed
21 Mutagenesis, extracellular low pH, intracellular low pH, pH sensitivity.

22

23

24 **Introduction**

25 Transient receptor potential channels (TRP channels) are membrane proteins that facilitate
26 the interpretation of external stimuli, and allow organisms to readily sense the environment
27 (Clapham 2003). These stimuli include temperature (Vandewauw et al. 2018; Brauchi and
28 Orio 2011), voltage (Clapham 2003; Brauchi and Orio 2011; Montell et al. 1985),
29 mechanical force (osmolarity (Strotmann et al. 2000; Liedtke and Friedman 2003; Quallo
30 et al. 2015), pressure (Suzuki et al. 2003), stretch (Strotmann et al. 2000; Hardie and Franze
31 2012; Maroto et al. 2005), gravity (Sun et al. 2009)), light (Montell et al. 1985; Minke
32 1977; Hardie 2014), proton concentration (Gerdes et al. 2007; Chandrashekar et al. 2006;
33 Semtner et al. 2007), and various chemical signals (Caterina et al. 1997; McKemy,
34 Neuhauser, and Julius 2002; Everaerts et al. 2011). TRP channels form homomeric or
35 heteromeric cation channels that can be selective or non-selective to cations; and most of
36 the TRP members are permeable to Ca^{2+} (Pan, Yang, and Reinach 2011). Upon activation,
37 TRP channels change membrane potential or intracellular calcium concentration ($[\text{Ca}^{2+}]_i$)
38 to promote downstream signal transductions. Depending on sequence homology and
39 channel architecture, TRP channels are divided into seven subfamilies, namely, TRPA
40 (Ankyrin), TRPC (Canonical), TRPM (Melastatin), TRPML (Mucolipin), TRPP
41 (Polycystin), TRPV (Vanilloid), and TRPN (NompC, no vertebrate member). 27 vertebrate
42 members of these subfamilies are expressed in humans (Venkatachalam and Montell 2007;
43 Uchida et al. 2019).

44 TRPM3 belongs to the subfamily of TRPM (Melastatin). TRPM3 is a non-selective
45 cation channel that is permeable to Ca^{2+} , Na^+ , Mn^{2+} and Mg^{2+} ions with a permeability ratio
46 of $P_{\text{Ca}}/P_{\text{Na}}$ of 1.57 ± 0.31 (Grimm et al. 2003). RT-qPCR analyses have shown expression

47 of human (hTRPM3), mouse (mTRPM3) and rat (rTRPM3) TRPM3 in a variety of tissues,
48 with the most abundant expression in the brain, kidney, pituitary gland and adipose tissues
49 (Oberwinkler and Philipp 2014; Zamudio-Bulcock et al. 2011). In sensory neurons,
50 TRPM3 functions as a noxious heat sensor; TRPM3 deficient mice lack the normal
51 response to noxious heat and do not develop inflammatory heat hyperalgesia (Vandewauw
52 et al. 2018; Vriens et al. 2011). Vangeel et al. recently demonstrated functional expression
53 of TRPM3 in human sensory neurons; where a large subset of nociceptor neurons express
54 TRPM3, and TRPM3 has been suggested to be a potential drug target for novel analgesics
55 (Vangeel et al. 2020; Moran and Szallasi 2018). Although, role of TRPM3 in central
56 nervous system has not been explored in detail yet, a recent study has shown high-level
57 expression of TRPM3 in mouse CA2 and CA3 hippocampal neurons and in the dentate
58 gyrus. Field potential recordings also showed that TRPM3 agonists inhibit synaptic
59 transmission and plasticity, and reduce long-term potentiation (LTP) in mouse
60 hippocampus (Held et al. 2020). Moreover, human genetic analyses have linked TRPM3
61 mutations with intellectual disability, epilepsy, inherited cataract and glaucoma (Dyment
62 et al. 2019; Bennett et al. 2014). In cardiovascular system, TRPM3 localizes in the
63 perivascular nerves of mouse mesenteric arteries, and induces vasodilation by stimulating
64 CGRP (calcitonin gene-related peptide) receptors (Alonso-Carbajo et al. 2019). TRPM3
65 forms homomultimeric channels, which are constitutively active (Grimm et al. 2003). In
66 addition, TRPM3 channel can also be activated by endogenous neurosteroid pregnenolone
67 sulfate (PS), nifedipine, and clotrimazole. Mefenamic acid, diclofenac, progesterone and
68 favanones have been reported to inhibit TRPM3 (Wagner et al. 2008; Uchida et al. 2019).
69 PS has been shown to increase neurotransmitter release, strengthen synaptic transmission

70 and modulate synaptic plasticity (Smith, Gibbs, and Farb 2014). However, whether
71 TRPM3 contribute to any of these neuronal functions of PS or not, is not clear (Zamudio-
72 Bulcock et al. 2011). One study has shown that PS-induced potentiation of spontaneous
73 glutamate release in Purkinje neurons of developing rats is mediated by TRPM3 (Zamudio-
74 Bulcock et al. 2011). In non-neuronal cells, PS upregulates activator protein 1 (AP-1) and
75 early growth response protein 1 (Egr-1) transcriptional activity, which can be blocked by
76 TRPM3 antagonists (Lesch, Rubil, and Thiel 2014). TRPM3 also upregulates c-Jun and c-
77 Fos promoter activity and stimulates CRE-controlled reporter gene transcription in
78 insulinoma and pancreatic β -cells, in a TRPM3-dependent manner (Muller, Rossler, and
79 Thiel 2011). In vascular smooth muscle cells, PS increases $[Ca^{2+}]_i$ and modulates
80 contractile responses, which can be inhibited by TRPM3 inhibitors (Naylor et al. 2010).
81 PS also increases $[Ca^{2+}]_i$ in fibroblast-like synoviocytes and suppresses the secretion of
82 hyaluronan via TRPM3 (Ciurtin et al. 2010).

83 Extracellular and intracellular protons modulate ion channel activity. For example,
84 extracellular acidification activates acid-sensing ion channels (ASICs), G-protein coupled
85 inward rectifier K^+ channels, nifedipine sensitive L-type Ca^{2+} channels, and acid-sensitive
86 Cl^- channels; while inhibiting two-pore domain K^+ channels (TASK-1, TASK-2, TASK-3,
87 TALK-1, and TALK-2), and reducing potency of ionotropic purinoceptors - P2X1, P2X3,
88 P2X4 and P2X7. Intracellular acidosis activates inward rectifier K^+ channel family protein
89 Kir6.1, K2p channel TREK-1 and TREK-2; however, Kir1.1, Kir4.1, and Kir5.1 activity
90 is inhibited by both intracellular and extracellular decreases in pH. Gap junction channels,
91 connexins, are also inhibited by intracellular acidosis. In addition, both intracellular and
92 extracellular acidification block the K2p channel TRESK, as well as depress or inhibit

93 TWIK-1 and TWIK-2. Some of the ion channels, such as, TASK-2, TRESK, TALK-1, and
94 TALK-2, which are blocked at low pH can be activated or gated open by alkalization.
95 Protons cannot activate or inhibit P2X2 and P2X5 homomultimers but decreases potency
96 and efficacy of ATP gating of P2X5, and sensitizes P2X2 receptors to ATP. To make things
97 even complex, protons can have a variable effect depending on the subunit composition of
98 heteromeric ion channels (Holzer 2009). TRP channels are no exception regarding variable
99 activity in response to pH. Specifically, TRPV1, TRPV4, and TRPC4 are activated by a
100 reduction of pH. In contrast, TRPC5 currents are increased by an acidic pH until 6.0 is
101 reached, at which point further decreases in pH reduce current (Holzer 2009). PKD2L1
102 (TRPP2) expressing neurons show action potentials in response to citric acid (Huang et al.
103 2006), whereas intracellular and extracellular pH inhibits TRPM2 (Du, Xie, and Yue
104 2009). Yet very little is known about how pH regulates TRPM3. Thus, to understand the
105 role of pH on TRPM3 activity, we studied how TRPM3 activation by PS responds to
106 different extracellular and intracellular pH conditions. In all experiments, we activated
107 TRPM3 by external application of PS, and all subsequent mentions of TRPM3 activity in
108 this manuscript must be considered as TRPM3 activity in response to PS, and not TRPM3
109 constitutive activity. As PS induced TRPM3 currents are almost two orders of magnitude
110 higher than TRPM3 constitutive currents (Wagner et al. 2008; Grimm et al. 2003; Lee et
111 al. 2003), we concluded that for our experiments, it is reasonable to exclude the effects of
112 constitutive TRPM3 activity.

113

114

115

116 **Materials & Methods**

117 **Plasmid and molecular biology**

118 The cDNA of human TRPM3 channel (accession number AJ505026) with C-terminal GFP
119 tag was provided by C. Harteneck (University of Tübingen, Tübingen, Germany) (Grimm
120 et al. 2003). Alternative splicing patterns of TRPM3 is highly conserved across human and
121 rodents (Oberwinkler et al. 2005). To date, 25 isoforms of mTRPM3 protein have been
122 identified, including a recently discovered variant - TRPM3 γ 3. Splicing events affect exons
123 8, 13, 15, 17, 20, 24 and 28 of TRPM3. α variants lack exon 2, β variants lack exon 1, and
124 γ variants lack a large part of exon 28 (Uchida et al. 2019; Oberwinkler and Philipp 2014).
125 Our hTRPM3 cDNA contains all 30 exons, where 389 amino acids in exon 28 has been
126 replaced with alternative carboxy terminus of 7 residues; this truncation does not affect any
127 functional activity of the ion channel (Oberwinkler and Philipp 2014; Grimm et al. 2003).
128 Mutations of hTRPM3-GFP were generated by site-directed mutagenesis (performed by
129 GENEWIZ Inc). The predicted mutations were verified by sequencing analysis.

130

131 **Cell culture and overexpression of hTRPM3-GFP and the mutants in HEK-293 cells.**

132 Human embryonic kidney (HEK) 293 cells were used to transiently overexpress wild-type
133 hTRPM3-GFP and its mutants. The cells were grown in DMEM/F12 medium (Fisher
134 Scientific, catalog no. MT10090CV) supplemented with 10% bovine growth serum
135 (HyClone, catalog no. SH30541.03), 100 U/ml penicillin / 100 mg/ml streptomycin (Fisher
136 Scientific, catalog no. SV30010) at 37°C in a 5% CO₂- controlled, humidity-controlled
137 incubator. Lipofectamine 2000 (Thermo Fisher Scientific, catalog no. 18324012) was used
138 for the transfection of TRPM3 into the cells in a 35-mm culture dish according to the

139 manufacturer's instructions. Successfully transfected cells were identified by their fused
140 GFP when illuminated at 480 nm excitation wavelength. Electrophysiological recordings
141 were conducted between 36- and 48-hours post-transfection.

142

143 **Electrophysiology**

144 All patch-clamp experiments were performed at room temperature (20–22°C). TRPM3
145 whole-cell currents were recorded using an Axopatch 200B amplifier. Data were digitized
146 at 10 kHz and digitally filtered offline at 5 kHz. Patch electrodes were pulled by Sutter P-
147 97 micropipette puller and fire-polished to resistance of 3-5 MΩ when filled with internal
148 solutions. Series resistance (Rs) was compensated up to 90% to reduce series resistance
149 errors to <5 mV. Cells in which Rs was >8 MΩ were discarded (Du, Xie, and Yue 2009).
150 For whole-cell current recording, ramp voltage stimuli (250 ms duration) were delivered
151 at 1-second intervals and the ranging from –100 to +100 mV. The internal pipette solution
152 for whole-cell current recordings contained (in mM): 115 Cs-methanesulfonate
153 (CsSO₃CH₃), 8 NaCl, 10 Cs-EGTA, 5 Na₂-ATP and 10 HEPES, with pH adjusted to 7.2
154 with CsOH. In high intracellular Ca²⁺ experiments, 0.93 mM CaCl₂ was added to the
155 above-mentioned intracellular solution and EGTA was reduced to 1 mM, resulting in 1 μM
156 free intracellular Ca²⁺. MaxChelator ([https://somapp.ucdmc.ucdavis.edu/ pharmacology/](https://somapp.ucdmc.ucdavis.edu/pharmacology/bers/maxchelator/downloads.htm)
157 [bers/maxchelator/downloads.htm](https://somapp.ucdmc.ucdavis.edu/pharmacology/bers/maxchelator/downloads.htm)) software from the University of California, Davis was
158 used to calculate free [Ca²⁺]_i.

159 To avoid proton activated chloride currents conducted by endogenous anion channels of
160 HEK-293 cells (Lambert and Oberwinkler 2005), NaCl in standard Tyrode solution was
161 replaced with Na-glutamate for all whole-cell current recordings. This external solution

162 contained (in mM): 145 Na-glutamate, 5 KCl, 2 CaCl₂, 1 MgCl₂, 10 HEPES, and 10
163 glucose, with pH adjusted to 7.4 with glutamic acid. Internal and external acidic pH
164 solutions were prepared as described previously with slight modifications (Du, Xie, and
165 Yue 2009). In brief, 10 mM HEPES used in the solutions at pH 7.4 and 7.0 was replaced
166 by 10 mM MES for the solutions at pH ≤ 6.0. Bath solutions containing 1 mM to 60 mM
167 NH₄Cl were prepared by decreasing Na⁺ concentrations to 85 mM in the solution to keep
168 the osmolarity constant, and osmolarity was adjusted to 300 ± 10 mOsm with mannitol. In
169 experiments designed to test protons permeability of TRPM3, pipette solutions contained
170 (in mM): 120 NMDG, 108 glutamic acid, 10 HEPES, 10 EGTA, with pH adjusted to 7.2
171 with NMDG. External solutions for proton permeability test contained (in mM): 145
172 NMDG, 10 HEPES and 10 Glucose; and pH was adjusted with glutamic acid. To prepare
173 the pH 5.5 external solution for proton permeability, 10 mM HEPES was replaced with 10
174 mM MES. PS was dissolved in DMSO to prepare 100 mM stock solution, and adequate
175 volume of stock PS solution was added to the external solution to achieve required
176 concentration. All the chemicals used in electrophysiological experiments were from
177 Sigma-Aldrich.

178

179 **Data analysis**

180 Statistical data were analyzed using GraphPad Prism 8. Pooled data are presented as mean
181 ± SEM. Concentration-response curves were fitted by an equation of the form: $E =$
182 $E_{max}\{1/[1+(IC_{50}/C)^n]\}$ where E is the effect at concentration C , E_{max} is the maximal effect,
183 IC_{50} is the concentration for half-maximal effect, and n is the Hill coefficient (Du, Xie, and
184 Yue 2009). Concentration of proton required for half-maximal inhibition is denoted by IC_{50}

185 (when H^+ concentration is expressed as molar concentration) and pH_{50} (when H^+
186 concentration is expressed by pH value). Statistical comparison of two groups was
187 performed by unpaired Student's t-test, $p < 0.05$ was considered statistically significant.
188 Statistical comparison of three or more groups was performed by one-way ANOVA with
189 Tukey's post hoc multiple comparison.

190

191 **Results**

192 **Extracellular and intracellular acidic pH inhibit TRPM3**

193 We studied the effects of low pH on TRPM3 by overexpressing hTRPM3-GFP in HEK-
194 293 cells and recording whole-cell currents in response to PS. We found that low
195 extracellular pH inhibits TRPM3, in a reversible manner (Fig. 1, A - D). To avoid proton
196 activated endogenous anion channel conducted chloride currents, external Cl^- was replaced
197 by glutamate (See Methods). Inhibitory effect of low extracellular pH (pH_o) was only
198 observed below pH 6.0. Specifically, at pH_o 7.0 and 6.0, recorded TRPM3 currents were
199 equivalent to pH_o 7.4 ($p > 0.05$ in both groups). At a pH_o below 6.0, acidic conditions
200 exhibited significant inhibition of TRPM3 (Fig. 1). pH_o 5.5, caused ~ 60% reduction in
201 TRPM3 whole-cell current induced by PS. Fitting these data in a non-linear regression
202 curve did not result in a well-fitted curve; we did not observe a concentration-dependent
203 effect of extracellular pH on TRPM3 activity. This might suggest an indirect inhibition of
204 TRPM3 by low pH_o . In addition, as shown in Fig. 1A, application of low extracellular pH
205 ($pH \leq 5.5$) with PS produced an initial activation of TRPM3 before blocking it. This
206 suggested that the onset of low pH_o inhibition is slower than the PS activation, supporting
207 the hypothesis that the inhibition of TRPM3 by low pH_o is indirect. We thus hypothesized

208 that protons block TRPM3 by permeating through TRPM3 and binding on a cytoplasmic
209 site. To test this hypothesis, we first investigated the effects of intracellular low pH (pH_i)
210 on TRPM3. Whole-cell TRPM3 currents were recorded using the low-pH pipette solutions
211 (see experimental procedures), while keeping extracellular pH constant at 7.4 (Fig. 2). Low
212 pH_i markedly reduced TRPM3 current in a concentration-dependent manner with a pH_{50}
213 value of 6.90 ± 0.11 (outward current at +100mV) (Fig. 2C) and pH_{50} value of 6.90 ± 0.15
214 (inward current at -100mV) (Fig. 2D). There was no significant difference in the steady-
215 state inhibition between inward and outward currents, concluding that there are no voltage-
216 dependent effects of acidic pH_i on inward and outward TRPM3 currents (Fig. 2, C and D).
217 To investigate the extent of modulation of TRPM3 by protons, we also introduced higher
218 pH_i than the physiological pH_i of 7.2. Recorded TRPM3 current plateaued at about pH_i 7.6.
219 Protons had similar inhibitory effects on both outward and inward TRPM3 currents (Fig.
220 2, A and B). Combined, our findings that pH_o 6.0 did not affect TRPM3 current but low
221 pH_i had an inhibitory pH_{50} value of 6.9, suggested a higher pH sensitivity of TRPM3 in the
222 cytoplasmic side.

223

224 **Effect of low pH_i on concentration-dependence of TRPM3 activation by PS**

225 PS binds directly to the extracellular side of the TRPM3 channel to activate it. TRPM3
226 channel stays both functional and unaffected by the presence of intracellular PS (Wagner
227 et al. 2008). Previous studies have shown that PS activates TRPM3 in a concentration-
228 dependent manner with an EC_{50} value of 12 μM and 23 μM for outward and inward current
229 respectively (Wagner et al. 2008). To investigate the effect of protons on PS concentration-
230 dependence of TRPM3, we perfused the cells with a wide range of PS concentrations (1

231 μM - 500 μM), while keeping pH_i constant at 7.2 or 6.0. TRPM3 whole-cell outward and
232 inward currents showed very similar PS concentration-dependence in both pH_i conditions
233 (Fig. 3). EC_{50} values for outward currents were 16 μM (pH_i 7.2) and 15 μM (pH_i 6.0) (Fig.
234 3D), and for inward currents were 21 μM (pH_i 7.2) and 26 μM (pH_i 6.0) (Fig. 3F). All
235 concentration-dependent curves plateaued after 50 μM PS stimulations (Fig. 3). We
236 observed a downward shift of the outward current ratio curve in response to low pH_i (Fig.
237 3C). However, when currents were normalized to the maximum TRPM3 activation by 500
238 μM PS, the outward current curve did not deviate in response to low pH_i (Fig. 3D). These
239 results indicate that higher proton concentration inside the cell reduces TRPM3 maximal
240 activation potential at any given PS concentration but does not affect PS concentration-
241 dependent activation of TRPM3. The PS concentration-dependent curve of TRPM3 inward
242 currents did not show any change in response to low pH_i (Fig. 3, E and F). In summary,
243 these data suggest that intracellular protons do not compete with PS for binding sites.

244

245 **TRPM3 inhibition by protons can be reversed by increasing pH_i**

246 Extracellular application of NH_4Cl produces a rise in pH_i resulting from an influx of NH_3 .
247 NH_3 binds intracellular protons and causes alkalization inside the cells (Jacobs 1922;
248 Warburg 1922). We observed that protons blocked TRPM3 from the cytoplasmic side,
249 thus we tested whether raising pH_i by applying NH_4Cl could rescue the TRPM3 current.
250 We perfused the cells with solutions where part of NaCl was replaced by an equal amount
251 of NH_4Cl (see experimental procedures), to test whether increasing pH_i while keeping
252 extracellular pH the same can reverse the blocking effects of protons on TRPM3. As shown
253 in Fig. 4, A and B, 30mM NH_4Cl increased recorded TRPM3 currents significantly. We

254 attribute this increase to the influx of NH_3 into the cell and removing bound protons from
255 the TRPM3 cytoplasmic side. Overall, this result substantiates our finding that TRPM3 is
256 blocked by protons binding to an intracellular site. Different concentrations of NH_4Cl were
257 applied to the same cell, and all NH_4Cl applications change intracellular pH. To confirm
258 that every TRPM3 stimulation starts at the same initial pH_i , we allowed adequate washing
259 time between two consecutive NH_4Cl + PS applications.

260 Subsequently, we wanted to test whether external NH_4Cl exhibits a concentration
261 dependent rescuing effect on TRPM3 activity or not. We perfused hTRPM3-GFP
262 overexpressed HEK-293 cells with modified Tyrode solutions containing different
263 concentrations of NH_4Cl (1 - 60 mM). Na^+ concentrations in all solutions were kept the
264 same, and osmolarities were adjusted to 300 ± 10 mOSM with Mannitol. We observed a
265 5-fold increase in TRPM3 activity at only 3 mM (NH_4Cl) concentration. Even 1 mM
266 NH_4Cl rescued some TRPM3 activity ($p < 0.05$). NH_4Cl concentrations higher than 3 mM
267 had higher impact on TRPM3 activity than 3 mM NH_4Cl . Although, when compared with
268 3 mM NH_4Cl , some of these higher concentrations showed significant increase in TRPM3
269 activity, there were no substantial increase in TRPM3 activity by further increase in NH_4Cl
270 concentration. This data indicates that TRPM3 activity is highly sensitive to intracellular
271 pH changes, at least at the intracellular pHs over 6.0. It is noteworthy that we did not
272 measure exact pH_i changes following external NH_4Cl applications, so the pH_i differences,
273 before and after NH_4Cl applications, are unknown here. However, these experiments still
274 substantiate our claim that TRPM3 activity is highly sensitive to intracellular pH changes,
275 at least at physiological pH_i ranges (pH_i 6.0 to 8.0). In this experiment, TRPM3 current
276 recordings from each cell spanned over 20 minutes period. To confirm that subsequent

277 application of NH₄Cl and PS for a long time does not affect TRPM3 activity, we also tested
278 individual cells with only one exposure to NH₄Cl, at different concentrations. The results
279 of these experiments are summarized in Supplementary Fig. 1 (sFig. 1). When compared
280 with TRPM3 currents from our earlier experiments (Fig. 4, D), where the same cells were
281 perfused with different concentrations of NH₄Cl, individual cells did not show a difference
282 (sFig. 1B). We also observed a higher increase in inward current than corresponding the
283 outward current (Fig. 4, I). The ratio of inward current to outward current increased from
284 0.13 at 1mM NH₄Cl to 0.54 at 60mM NH₄Cl. This increase was consistent with the result
285 obtained from individual cells (sFig. 1).

286

287 **TRPM3 is potentially permeable to protons**

288 For a better understanding of the proton inhibition of TRPM3, we hypothesized that
289 protons permeate through TRPM3 when it is activated by PS. The lipid bilayer (*e.g.* cell
290 membrane) presents a strong barrier for the transport of charged ions through eukaryotic
291 cell membranes. Although the permeability of protons is higher than other monovalent
292 cations, which can partially be explained by the presence of transient water wires or long-
293 lived hydrophilic pores (Tepper and Voth 2005), it is unlikely that these mechanisms can
294 transport sufficient protons across the membrane to have a direct impact on an
295 overexpressed protein, unless protons are passing through the overexpressed ion-channel
296 itself. We thus examined whether protons can permeate through TRPM3. We recorded
297 TRPM3 inward current in HEK-293 cells, overexpressing hTRPM3-GFP, by holding the
298 membrane at -100mV and applying PS and low pH solutions from the outside. We
299 maintained pH_i at 7.6 to provide a higher concentration gradient for protons. All cations

300 except protons were removed using NMDG in external and internal solutions. PS, along
301 with NMDG pH 5.5 extracellular solution, produced a small transient inward current in
302 TRPM3 transfected HEK-293 cells (Fig. 5). Indeed, the amplitude of this current is
303 significantly lower than TRPM3 currents observed in our whole-cell recordings. This is
304 because in this experiment, all cations have been removed besides a limited amount of H⁺.
305 extracellular and intracellular proton concentrations was 3.2×10^{-3} mM (pH 5.5) and 2.5
306 $\times 10^{-5}$ mM (pH 7.6) respectively. These concentrations represent the total cation
307 concentrations of these solutions, which are several orders of magnitude lower than the
308 total cation concentrations of our modified Tyrode solutions. In addition, extracellular pH
309 5.5 blocks about 60% of TRPM3 currents. However, to provide a reasonable proton
310 gradient across the cell membrane, it is critical to conduct this experiment at a low
311 extracellular pH. Since, there were no other cation involved, although low in amplitude,
312 this current suggests passage of proton through TRPM3 channel. In addition, the proton
313 current is transient is because of the intracellular inhibitory effects of H⁺ on TRPM3 after
314 its permeation. Mock transfected cells did not produce any inward current in response to
315 PS (Data not shown). This evidence indicates that TRPM3 is potentially permeable to
316 proton.

317

318 **The inhibition of intracellular Ca²⁺ on TRPM3 is pH independent**

319 TRPM3 displays higher permeability for divalent cations than monovalent cations. For the
320 splice variant TRPM3 α 2, 24% of total TRPM3 current is expected to result from Ca²⁺
321 (Przibilla et al. 2018), suggesting a large increase in [Ca²⁺]_i following TRPM3 activation.
322 Multiple studies verified this effect showing an increase in [Ca²⁺]_i in a micromolar range

323 following TRPM3 activation (Vriens et al. 2011; Straub et al. 2013; Przibilla et al. 2018).
324 A recent study demonstrated that an increase in $[Ca^{2+}]_i$, independent of TRPM3 activity,
325 inhibits TRPM3 in a calmodulin-dependent manner (Przibilla et al. 2018). This suggests a
326 potential negative feedback mechanism that regulates a high increase in $[Ca^{2+}]_i$ resulting
327 from TRPM3 activation. Studies conducted by others enlist $[Ca^{2+}]_i$ as a regulator of
328 TRPM3 activity. In our study, we found that intracellular proton blocks TRPM3 as well..
329 Hence, we asked the question, how do these two regulatory mechanisms interact with each
330 other? To find the effect of $[Ca^{2+}]_i$ on the concentration-dependent inhibition of TRPM3 by
331 protons, we tested TRPM3 activity in two different $[Ca^{2+}]_i$ conditions, while providing a
332 wide range of pH_i , using whole-cell patch clamp of TRPM3 transfected cells. In addition
333 to the inhibition of TRPM3 current by $[Ca^{2+}]_i$ observed by J. Przibilla et al., we observed
334 an additional delayed inhibition of TRPM3 current by Ca^{2+} . For example, under $1\mu M$
335 $[Ca^{2+}]_i$, recorded current showed a further inhibition after initial activation and the residual
336 current amplitudes were less than 50% of the initial activation (Fig 6, B and C). Low $[Ca^{2+}]_i$
337 (< 10 nM) did not show a delayed inhibition of TRPM3 current (Fig. 6A). pH_i
338 concentration-dependence of TRPM3 was not affected by $[Ca^{2+}]_i$, as they showed similar
339 pH_{50} Values (7.0 ± 0.1 , 7.1 ± 0.1 , 7.2 ± 0.5) for low $[Ca^{2+}]_i$, high Ca^{2+} initial and high Ca^{2+}
340 delayed current intensities (Fig. 6E). It is noteworthy that, despite having similar pH_{50}
341 values, TRPM3 outward current densities were significantly decreased in high $[Ca^{2+}]_i$
342 conditions (Fig. 6E). To investigate if protons affected the percentage of current inhibited
343 in delayed current intensities compared with the initial current intensities, we analyzed the
344 ratio of delayed to initial current intensities in different pH_i at high $[Ca^{2+}]_i$ concentration.
345 We did not observe any significant difference between the ratios resulting from different

346 pH_i (Fig. 6F). Overall, these results indicate that, although $[Ca^{2+}]_i$ inhibits TRPM3, it does
347 not affect the regulation of TRPM3 by intracellular protons.

348

349 **Molecular mechanism underlying TRPM3 inhibition by protons**

350 Glutamate, aspartate, histidine, and lysine residues are potential proton acceptors,
351 especially glutamate and aspartate, which present negative charges (Zhou and Pang 2018).

352 To identify the amino acid residues of TRPM3 accountable for its sensitivity to pH_i , we

353 prepared hTRPM3-GFP mutant plasmids having mutations in the pore region. We selected

354 all eight glutamate and aspartate amino acids, in the vestibule of the loop between S5 and

355 S6 transmembrane domains (Fig. 7A). These eight residues were either a glutamate and

356 aspartate amino acid, and they were mutated to glutamine. We created two double mutants

357 (E1034Q - E1035Q, E1072Q - D1073Q) and six single mutants (E1055Q, D1059Q,

358 D1062Q, E1069Q, E1072Q, and D1073Q). We expressed these mutants in HEK-293 cells

359 and recorded elicited currents in response to PS, while perfusing with physiological and

360 low pH external solutions (Fig. 7B). Except for E1055Q, which resulted in a non-functional

361 ion-channel, all other mutants exhibited identical I-V relation to WT-hTRPM3, although

362 most of the mutants showed markedly reduced current amplitudes (Fig. 7B). We perfused

363 cells expressing these mutants with external solutions of pH 7.4 and pH 5.5. The pH of 5.5

364 was selected as representative of low pH external solutions because at this pH, WT-TRPM3

365 currents were blocked significantly yet sufficient activity was maintained for analysis. We

366 compared the percent decrease in TRPM3 current from pH_o 7.4 to pH_o 5.5 for all the

367 mutants and WT-TRPM3 (Fig. 7C). The double mutant (E1034Q - E1035Q), E1069Q, and

368 E1072Q showed similar sensitivity to protons when compared with the WT-TRPM3.

369 Mutants D1059Q and D1062Q were found to be more sensitive to protons, as the reduction
370 of whole-cell current due to low pH_o was increased to 93.9% and 84.1% in D1059Q and
371 D1062Q, respectively, compared to 56.5% observed in WT-TRPM3. Mutant D1073Q
372 showed significantly less sensitivity towards protons, as pH_o 5.5 reduced its current
373 amplitude only by 25%. As summarized in Fig. 7C, these results establish the amino acid
374 residues D1059Q, D1062Q and D1073Q as some of the key determinants of protons
375 sensitivity in TRPM3. Although it is unclear at this moment why mutating these residues
376 produce variable effects (increased or decreased proton sensitivity), these data suggested
377 that the pore vestibule of TRPM3 is critical for the pH sensitivity. Further studies are
378 required to delineate the underlying mechanism of these variable effects.

379

380 **Discussion**

381 We demonstrated for the first time that TRPM3 is a proton-permeable channel regulated
382 by both extracellular and intracellular acidic conditions. Our experiments suggest a direct
383 interaction of intracellular protons with the cytoplasmic side of TRPM3 to induce a
384 blocking effect, whereas extracellular protons permeate through the ion-channel first to
385 block it from the intracellular side. We also demonstrated that the blocking effect of the
386 intracellular protons could be reversed by decreasing intracellular protons concentrations,
387 which indicates a reversible binding of protons to the intracellular amino acid residues. We
388 identified an internal residue responsible for protons sensitivity of TRPM3. Finally, we
389 demonstrated that low internal pH produces a downward shift of PS concentration-
390 dependent activation of TRPM3 by reducing the amplitude of TRPM3-mediated currents

391 at any given pH_o. Overall, we report evidence for the regulatory role of protons on TRPM3
392 activation and the molecular mechanism responsible for it.

393

394 **General characteristics of TRPM3**

395 TRPM3 is a heat-sensitive ion channel, which is expressed in a somatosensory neuron
396 where its role as a noxious heat sensor has been established (Vriens et al. 2011;
397 Vandewauw et al. 2018). Activation of pancreatic TRPM3 increases glucose-induced
398 insulin release (Wagner et al. 2008). These data indicate the existence of multiple TRPM3
399 regulatory molecules. Indeed, cytosolic phosphatidylinositol biphosphates (PIPs) and
400 ATP have a stimulatory effect on TRPM3. Activation of phospholipase C-coupled
401 muscarinic acetylcholine receptors inhibit recombinant and endogenous TRPM3 (Toth et
402 al. 2015). Calmodulin binds to multiple sites of TRPM3 in Ca²⁺-dependent manner, and
403 both intracellular calmodulin and Ca²⁺ inhibits TRPM3 (Holakovska et al. 2012; Przibilla
404 et al. 2018). Here we report the modulatory role of protons on TRPM3. Reversible
405 inhibition of TRPM3 by protons indicates that acidic pH may serve as a negative feedback
406 mechanism to regulate TRPM3 activity in physiological/pathological conditions.

407

408 **Regulations of pH on TRP channels**

409 Acidification has modulatory effects on variety of ion channels (discussed in the
410 introduction) including TRP channels. Extracellular acidic pH modulates TRPV1 channel
411 gating (Jordt, Tominaga, and Julius 2000; Ryu, Liu, and Qin 2003), stimulates TRPC4 and
412 TRPC5, but inhibits TRPC6 (Semtner et al. 2007), TRPM5 (Liu, Zhang, and Liman 2005),
413 and TRPV5 (Yeh et al. 2003), and potentiates TRPM6 and TRPM7 inward currents (Jiang,

414 Li, and Yue 2005; Li, Jiang, and Yue 2006; Li et al. 2007). Intracellular protons inhibit
415 TRPM7 (Kozak et al. 2005), and block TRPM8 (Andersson, Chase, and Bevan 2004). Here
416 we demonstrate that PS-induced TRPM3 outward and inward currents both are inhibited
417 by protons. Although both intracellular and extracellular acidic conditions inhibit TRPM3,
418 there are differences between internal and external proton-induced inhibition. Extracellular
419 protons cannot inhibit TRPM3 until pH reaches below 6.0, but pH_i has a pH_{50} value of 6.9.
420 We demonstrated a very sharp inhibition by protons at an external pH below 6.0; this
421 inhibition did not follow a typical concentration-response relationship. Whereas internal
422 protons efficiently blocked TRPM3 current and showed a concentration-response
423 relationship. These results suggest that protons are not competing with PS for the same
424 binding site of TRPM3, and indicated that TRPM3 may contain proton-binding sites in the
425 cytoplasmic domains. It is plausible that an increase in extracellular proton's concentration
426 causes protons influx through TRPM3 that enables protons to bind to its internal binding
427 site to inhibit TRPM3. To rule out the effects of proton-activated endogenous chloride
428 currents, we conducted all whole-cell recordings under very low intracellular and
429 extracellular Cl^- concentrations. Indeed, our external and internal solutions contained 8
430 mM Cl^- , but this concentration of protons is not capable of activating endogenous anions
431 channels of HEK293 cells (Lambert and Oberwinkler 2005).

432

433 **Mechanisms of effects of protons on TRPM3**

434 It appeared that extracellular pH (< 6.0) strongly blocks TRPM3 activities, which would
435 indicate TRPM3 is regulated by extracellular acidic pH directly. However, the lack of pH
436 concentration-dependent activity did not support this hypothesis. These findings led us to

437 the conclusion that protons do not have extracellular binding sites, at least under the
438 activations of PS. Reduced intracellular pH appeared to have clear pH concentration-
439 dependent effects on TRPM3, which begs the question: how might external protons affect
440 TRPM3 gating properties? The cell membrane must have a mechanism for the proton
441 permeation and thus change the intracellular pH. It is possible that protons cross the
442 TRPM3 while it is open, although we cannot exclude the possibility that protons may
443 permeate the cell membrane directly.

444 Our data suggests that protons directly cross TRPM3 when it is activated by PS.
445 Consistently, no proton current was found without activating TRPM3, supporting the
446 conclusion that TRPM3 is potentially permeable to protons. We also studied the regulation
447 of TRPM3 by Ca^{2+} . Previous studies have shown that TRPM3 is a Ca^{2+} permeable ion
448 channel (Grimm et al. 2003; Lee et al. 2003). TRPM3 channel activity strongly depends
449 on intracellular Ca^{2+} (Przibilla et al. 2018). Along with the inhibition of TRPM3 current
450 amplitude, we also found that Ca^{2+} accelerates the decay time of TRPM3. Increased $[\text{Ca}^{2+}]_i$
451 from minimum to $1\ \mu\text{M}$ significantly reduces the plateau of the current. In general, $[\text{Ca}^{2+}]_i$
452 is a key regulator to modulate the TRPM3 gating - we hoped to visualize the interaction
453 between $[\text{Ca}^{2+}]_i$ and protons. However, high $[\text{Ca}^{2+}]_i$ did not change the pH_{50} of the effects
454 of intracellular protons on TRPM3 (Fig. 6). Vice versa, decreased $[\text{H}^+]_i$ did not affect the
455 Ca^{2+} inhibition on TRPM3 (Fig. 6). Therefore, it appears unlikely that protons can inhibit
456 TRPM3 channel activities by competing with $[\text{Ca}^{2+}]_i$ for a binding site on the cytoplasmic
457 side.

458 To determine the molecular mechanism by which intracellular protons inhibit
459 TRPM3, we mutated all the titratable residues in the pore region between S5 and S6 to

460 determine which sites are responsible for pH_i sensitivity. Among most of the mutations of
461 Asp and Glu residues, three residues-D1059, D1062 and D1073-which we predicted to
462 locate in the inner vestibule in the pore region, strongly change the proton sensitivities. We
463 conclude these residues in the pore region could be the proton binding sites. Of course, we
464 should not exclude any other intracellular binding sites. For example, C terminus of the
465 S4-S5 linker is thought to be critical for changing TRP channel's pH_i sensitivity (Du, Xie,
466 and Yue 2009). Although, how intracellular protons change TRPM3 gating properties
467 through these residues is still unknown, it will be of interest to investigate whether acidic
468 intracellular pH alters intracellular signaling pathways in future studies. It will also be of
469 interest to investigate other potential proton binding sites that might interact with $[\text{Ca}^{2+}]_i$
470 near the intracellular mouth and act as the $[\text{Ca}^{2+}]_i$ -activating site to regulate $[\text{Ca}^{2+}]_i$
471 mediated TRPM3 activation. Further investigation is required to test this hypothesis.

472

473 **Conclusion**

474 Our findings suggest that cellular acidification serves as a negative or protective feedback
475 mechanism to limit TRPM3 activities. Although the development of intracellular acidosis
476 has not been well established, metabolic acidosis is a relatively common condition that
477 causes pH_i to fall (Salameh, Ruffin, and Boron 2014). Some reports suggest that during
478 metabolic acidosis, insulin secretion is depressed (Mak 1998; Bigner et al. 1996). Thus, it
479 is possible that a low pH-mediated dampening of TRPM3 activity might contribute to the
480 decreased insulin secretion observed in metabolic acidosis. If true, then modulating
481 TRPM3 activity might be a potential future clinical application in treating acidosis induced
482 pancreatic disorders.

483 Collectively, we show that external and internal acidic pH show strong and state-
484 dependent inhibition of the TRPM3 channels. Asp1073 residue in the inner vestibule of the
485 channel pore is critical in modulating this inhibition. Given the physiological significance
486 of TRPM3 in numerous cells, including pancreatic beta cells and sensory neurons,
487 understanding TRPM3 gating by protons may generate new physiological and/or
488 pathological insights.

489

490 **Acknowledgement**

491 We thank Dr. C. Harteneck for providing the TRPM3 construct. We thank Dr. Lixia Yue
492 for her suggestions and comments. We thank Dr. Boren Lin, Erin Koffman, Tyler Ortyl,
493 Farzaneh Naghavi, and Kritika Singh for their comments. J.D. is supported by the National
494 Institutes of Mental Health (5R01 MH113986). LRR is supported by the National Institutes
495 of Health (R00HL119560, OT2OD023854, OT2OD026582)

496

497 **Conflict of Interest**

498 The authors declare no conflict of interest.

499

500 **Author Contributions**

501 J.D. conceived and supervised the project. J.D., MZ.HS. and L.X. designed the experiments
502 with input from Y.S.L. and L.R.R. MZ.HS. and L.X. did most of the patch-clamp
503 experiments. Y.S.L. and L.R.R. performed molecular biology experiments and oversaw the
504 mutagenesis of TRPM3. MZ.HS. and J.D. drafted the manuscript with input from all
505 authors contributed to finalizing the manuscript.

506

507 **Abbreviations**

508 TRP: Transient Receptor Potential; TRPM: Melastatin-like TRP channels; GFP: Green
509 Fluorescent Protein; NMDG: N-methyl-D-glucamine; PS: Pregnenolone Sulfate;
510 pH_o : Extracellular pH; pH_i : Intracellular pH; AP-1: Activator Protein-1; Egr-1: Early
511 Growth Response protein 1; CRE: cAMP response element; K2p: Two-pore domain K^+
512 channels; TWIK: Tandem of pore domains in Weak Inward rectifier K^+ channels; TASK:
513 TWIK-related Acid-Sensitive K^+ channels; Kir: Inward rectifier K^+ channel; TREK:
514 TWIK-RElated K^+ channels; TRESK: TWIK-RElated spinal cord K^+ channels; TALK:
515 TWIK-related ALkaline pH-activated K^+ channels; ATP: Adenosine TriPhosphate;
516 PKD2L1: Polycystic Kidney Disease 2-Like ion channel-1; CGRP: Calcitonin Gene-
517 Related Protein.

518

519

520 **References**

521 Alonso-Carbajo, L., Y. A. Alpizar, J. B. Startek, J. R. Lopez-Lopez, M. T. Perez-Garcia,
522 and K. Talavera. 2019. 'Activation of the cation channel TRPM3 in perivascular
523 nerves induces vasodilation of resistance arteries', *J Mol Cell Cardiol*, 129: 219-
524 30.
525 Andersson, D. A., H. W. Chase, and S. Bevan. 2004. 'TRPM8 activation by menthol,
526 icilin, and cold is differentially modulated by intracellular pH', *J Neurosci*, 24:
527 5364-9.
528 Bennett, Thomas M., Donna S. Mackay, Carla J. Siegfried, and Alan Shiels. 2014.
529 'Mutation of the melastatin-related cation channel, TRPM3, underlies inherited
530 cataract and glaucoma', *PLoS One*, 9: e104000-e00.
531 Bigner, D. R., J. P. Goff, M. A. Faust, J. L. Burton, H. D. Tyler, and R. L. Horst. 1996.
532 'Acidosis effects on insulin response during glucose tolerance tests in Jersey
533 cows', *J Dairy Sci*, 79: 2182-8.
534 Brauchi, S., and P. Orío. 2011. 'Voltage sensing in thermo-TRP channels', *Adv Exp Med
535 Biol*, 704: 517-30.

- 536 Caterina, M. J., M. A. Schumacher, M. Tominaga, T. A. Rosen, J. D. Levine, and D.
537 Julius. 1997. 'The capsaicin receptor: a heat-activated ion channel in the pain
538 pathway', *Nature*, 389: 816-24.
- 539 Chandrashekar, J., M. A. Hoon, N. J. Ryba, and C. S. Zuker. 2006. 'The receptors and
540 cells for mammalian taste', *Nature*, 444: 288-94.
- 541 Ciurtin, C., Y. Majeed, J. Naylor, P. Sukumar, A. A. English, P. Emery, and D. J. Beech.
542 2010. 'TRPM3 channel stimulated by pregnenolone sulphate in synovial
543 fibroblasts and negatively coupled to hyaluronan', *BMC Musculoskelet Disord*,
544 11: 111.
- 545 Clapham, D. E. 2003. 'TRP channels as cellular sensors', *Nature*, 426: 517-24.
- 546 Du, Jianyang, Jia Xie, and Lixia Yue. 2009. 'Modulation of TRPM2 by acidic pH and the
547 underlying mechanisms for pH sensitivity', *The Journal of general physiology*,
548 134: 471-88.
- 549 Dyment, David A, Paulien A Terhal, Cecilie F Rustad, Kristian Tveten, Christopher
550 Griffith, Parul Jayakar, Marwan Shinawi, Sara Ellingwood, Rosemarie Smith, and
551 Koen van Gassen. 2019. 'De novo substitutions of TRPM3 cause intellectual
552 disability and epilepsy', *European Journal of Human Genetics*, 27: 1611-18.
- 553 Everaerts, W., M. Gees, Y. A. Alpizar, R. Farre, C. Leten, A. Apetrei, I. Dewachter, F.
554 van Leuven, R. Vennekens, D. De Ridder, B. Nilius, T. Voets, and K. Talavera.
555 2011. 'The capsaicin receptor TRPV1 is a crucial mediator of the noxious effects
556 of mustard oil', *Curr Biol*, 21: 316-21.
- 557 Gerdes, J. M., Y. Liu, N. A. Zaghloul, C. C. Leitch, S. S. Lawson, M. Kato, P. A.
558 Beachy, P. L. Beales, G. N. DeMartino, S. Fisher, J. L. Badano, and N. Katsanis.
559 2007. 'Disruption of the basal body compromises proteasomal function and
560 perturbs intracellular Wnt response', *Nat Genet*, 39: 1350-60.
- 561 Grimm, C., R. Kraft, S. Sauerbruch, G. Schultz, and C. Harteneck. 2003. 'Molecular and
562 functional characterization of the melastatin-related cation channel TRPM3', *J*
563 *Biol Chem*, 278: 21493-501.
- 564 Hardie, R. C. 2014. 'Photosensitive TRPs', *Handb Exp Pharmacol*, 223: 795-826.
- 565 Hardie, R. C., and K. Franze. 2012. 'Photomechanical responses in Drosophila
566 photoreceptors', *Science*, 338: 260-3.
- 567 Held, Katharina, Marie Mulier, Nele Van Ranst, Yang Ge, Thomas Voets, Yu Tian
568 Wang, and Joris Vriens. 2020. 'TRPM3 Inhibits Synaptic Transmission and
569 Plasticity in the Hippocampus', *Biophysical Journal*, 118: 21a.
- 570 Holakovska, B., L. Grycova, M. Jirku, M. Sulc, L. Bumba, and J. Teisinger. 2012.
571 'Calmodulin and S100A1 protein interact with N terminus of TRPM3 channel', *J*
572 *Biol Chem*, 287: 16645-55.
- 573 Holzer, Peter. 2009. 'Acid-sensitive ion channels and receptors', *Handbook of*
574 *experimental pharmacology*: 283-332.
- 575 Huang, Angela L., Xiaoke Chen, Mark A. Hoon, Jayaram Chandrashekar, Wei Guo,
576 Dimitri Tränkner, Nicholas J. P. Ryba, and Charles S. Zuker. 2006. 'The cells and
577 logic for mammalian sour taste detection', *Nature*, 442: 934-38.
- 578 Jacobs, M. H. 1922. 'The influence of ammonium salts on cell reaction', *J Gen Physiol*, 5:
579 181-8.
- 580 Jiang, J., M. Li, and L. Yue. 2005. 'Potentiation of TRPM7 inward currents by protons', *J*
581 *Gen Physiol*, 126: 137-50.

- 582 Jordt, S. E., M. Tominaga, and D. Julius. 2000. 'Acid potentiation of the capsaicin
583 receptor determined by a key extracellular site', *Proc Natl Acad Sci U S A*, 97:
584 8134-9.
- 585 Kozak, J. A., M. Matsushita, A. C. Nairn, and M. D. Cahalan. 2005. 'Charge screening by
586 internal pH and polyvalent cations as a mechanism for activation, inhibition, and
587 rundown of TRPM7/MIC channels', *J Gen Physiol*, 126: 499-514.
- 588 Lambert, S., and J. Oberwinkler. 2005. 'Characterization of a proton-activated, outwardly
589 rectifying anion channel', *J Physiol*, 567: 191-213.
- 590 Lee, N., J. Chen, L. Sun, S. Wu, K. R. Gray, A. Rich, M. Huang, J. H. Lin, J. N. Feder, E.
591 B. Janovitz, P. C. Levesque, and M. A. Blonar. 2003. 'Expression and
592 characterization of human transient receptor potential melastatin 3 (hTRPM3)', *J*
593 *Biol Chem*, 278: 20890-7.
- 594 Lesch, A., S. Rubil, and G. Thiel. 2014. 'Activation and inhibition of transient receptor
595 potential TRPM3-induced gene transcription', *Br J Pharmacol*, 171: 2645-58.
- 596 Li, M., J. Du, J. Jiang, W. Ratzan, L. T. Su, L. W. Runnels, and L. Yue. 2007. 'Molecular
597 determinants of Mg²⁺ and Ca²⁺ permeability and pH sensitivity in TRPM6 and
598 TRPM7', *J Biol Chem*, 282: 25817-30.
- 599 Li, M., J. Jiang, and L. Yue. 2006. 'Functional characterization of homo- and heteromeric
600 channel kinases TRPM6 and TRPM7', *J Gen Physiol*, 127: 525-37.
- 601 Liedtke, W., and J. M. Friedman. 2003. 'Abnormal osmotic regulation in *trpv4*^{-/-} mice',
602 *Proc Natl Acad Sci U S A*, 100: 13698-703.
- 603 Liu, D., Z. Zhang, and E. R. Liman. 2005. 'Extracellular acid block and acid-enhanced
604 inactivation of the Ca²⁺-activated cation channel TRPM5 involve residues in the
605 S3-S4 and S5-S6 extracellular domains', *J Biol Chem*, 280: 20691-9.
- 606 Mak, R. H. 1998. 'Effect of metabolic acidosis on insulin action and secretion in uremia',
607 *Kidney Int*, 54: 603-7.
- 608 Maroto, R., A. Raso, T. G. Wood, A. Kurosky, B. Martinac, and O. P. Hamill. 2005.
609 'TRPC1 forms the stretch-activated cation channel in vertebrate cells', *Nat Cell*
610 *Biol*, 7: 179-85.
- 611 McKemy, D. D., W. M. Neuhausser, and D. Julius. 2002. 'Identification of a cold
612 receptor reveals a general role for TRP channels in thermosensation', *Nature*, 416:
613 52-8.
- 614 Minke, B. 1977. 'Drosophila mutant with a transducer defect', *Biophys Struct Mech*, 3:
615 59-64.
- 616 Montell, C., K. Jones, E. Hafen, and G. Rubin. 1985. 'Rescue of the Drosophila
617 phototransduction mutation *trp* by germline transformation', *Science*, 230: 1040-3.
- 618 Moran, M. M., and A. Szallasi. 2018. 'Targeting nociceptive transient receptor potential
619 channels to treat chronic pain: current state of the field', *Br J Pharmacol*, 175:
620 2185-203.
- 621 Muller, I., O. G. Rossler, and G. Thiel. 2011. 'Pregnenolone sulfate activates basic region
622 leucine zipper transcription factors in insulinoma cells: role of voltage-gated Ca²⁺
623 channels and transient receptor potential melastatin 3 channels', *Mol Pharmacol*,
624 80: 1179-89.
- 625 Naylor, J., J. Li, C. J. Milligan, F. Zeng, P. Sukumar, B. Hou, A. Sedo, N. Yuldasheva, Y.
626 Majeed, D. Beri, S. Jiang, V. A. Seymour, L. McKeown, B. Kumar, C. Harteneck,
627 D. O'Regan, S. B. Wheatcroft, M. T. Kearney, C. Jones, K. E. Porter, and D. J.

- 628 Beech. 2010. 'Pregnenolone sulphate- and cholesterol-regulated TRPM3 channels
629 coupled to vascular smooth muscle secretion and contraction', *Circ Res*, 106:
630 1507-15.
- 631 Oberwinkler, J., A. Lis, K. M. Giehl, V. Flockerzi, and S. E. Philipp. 2005. 'Alternative
632 splicing switches the divalent cation selectivity of TRPM3 channels', *J Biol*
633 *Chem*, 280: 22540-8.
- 634 Oberwinkler, J., and S. E. Philipp. 2014. 'TRPM3', *Handb Exp Pharmacol*, 222: 427-59.
- 635 Pan, Z., H. Yang, and P. S. Reinach. 2011. 'Transient receptor potential (TRP) gene
636 superfamily encoding cation channels', *Hum Genomics*, 5: 108-16.
- 637 Przibilla, J., S. Dembla, O. Rizun, A. Lis, M. Jung, J. Oberwinkler, A. Beck, and S. E.
638 Philipp. 2018. 'Ca(2+)-dependent regulation and binding of calmodulin to
639 multiple sites of Transient Receptor Potential Melastatin 3 (TRPM3) ion
640 channels', *Cell Calcium*, 73: 40-52.
- 641 Quallo, T., N. Vastani, E. Horridge, C. Gentry, A. Parra, S. Moss, F. Viana, C. Belmonte,
642 D. A. Andersson, and S. Bevan. 2015. 'TRPM8 is a neuronal osmosensor that
643 regulates eye blinking in mice', *Nat Commun*, 6: 7150.
- 644 Ryu, S., B. Liu, and F. Qin. 2003. 'Low pH potentiates both capsaicin binding and
645 channel gating of VR1 receptors', *J Gen Physiol*, 122: 45-61.
- 646 Salameh, A. I., V. A. Ruffin, and W. F. Boron. 2014. 'Effects of metabolic acidosis on
647 intracellular pH responses in multiple cell types', *Am J Physiol Regul Integr Comp*
648 *Physiol*, 307: R1413-27.
- 649 Semtner, M., M. Schaefer, O. Pinkenburg, and T. D. Plant. 2007. 'Potentiation of TRPC5
650 by protons', *J Biol Chem*, 282: 33868-78.
- 651 Smith, C. C., T. T. Gibbs, and D. H. Farb. 2014. 'Pregnenolone sulfate as a modulator of
652 synaptic plasticity', *Psychopharmacology (Berl)*, 231: 3537-56.
- 653 Straub, I., U. Krugel, F. Mohr, J. Teichert, O. Rizun, M. Konrad, J. Oberwinkler, and M.
654 Schaefer. 2013. 'Flavanones that selectively inhibit TRPM3 attenuate thermal
655 nociception in vivo', *Mol Pharmacol*, 84: 736-50.
- 656 Strotmann, R., C. Harteneck, K. Nunnenmacher, G. Schultz, and T. D. Plant. 2000.
657 'OTRPC4, a nonselective cation channel that confers sensitivity to extracellular
658 osmolarity', *Nat Cell Biol*, 2: 695-702.
- 659 Sun, Y., L. Liu, Y. Ben-Shahar, J. S. Jacobs, D. F. Eberl, and M. J. Welsh. 2009. 'TRPA
660 channels distinguish gravity sensing from hearing in Johnston's organ', *Proc Natl*
661 *Acad Sci U S A*, 106: 13606-11.
- 662 Suzuki, M., A. Mizuno, K. Kodaira, and M. Imai. 2003. 'Impaired pressure sensation in
663 mice lacking TRPV4', *J Biol Chem*, 278: 22664-8.
- 664 Tepper, H. L., and G. A. Voth. 2005. 'Protons may leak through pure lipid bilayers via a
665 concerted mechanism', *Biophys J*, 88: 3095-108.
- 666 Toth, B. I., M. Konrad, D. Ghosh, F. Mohr, C. R. Halaszovich, M. G. Leitner, J. Vriens,
667 J. Oberwinkler, and T. Voets. 2015. 'Regulation of the transient receptor potential
668 channel TRPM3 by phosphoinositides', *J Gen Physiol*, 146: 51-63.
- 669 Uchida, K., N. Fukuta, J. Yamazaki, and M. Tominaga. 2019. 'Identification and
670 classification of a new TRPM3 variant (gamma subtype)', *J Physiol Sci*, 69: 623-
671 34.

- 672 Vandewauw, I., K. De Clercq, M. Mulier, K. Held, S. Pinto, N. Van Ranst, A. Segal, T.
673 Voet, R. Vennekens, K. Zimmermann, J. Vriens, and T. Voets. 2018. 'A TRP
674 channel trio mediates acute noxious heat sensing', *Nature*, 555: 662-66.
- 675 Vangeel, L., M. Benoit, Y. Miron, P. E. Miller, K. De Clercq, P. Chaltin, C. Verfaillie, J.
676 Vriens, and T. Voets. 2020. 'Functional expression and pharmacological
677 modulation of TRPM3 in human sensory neurons', *Br J Pharmacol*.
- 678 Venkatachalam, Kartik, and Craig Montell. 2007. 'TRP channels', *Annual review of*
679 *biochemistry*, 76: 387-417.
- 680 Vriens, J., G. Owsianik, T. Hofmann, S. E. Philipp, J. Stab, X. Chen, M. Benoit, F. Xue,
681 A. Janssens, S. Kerselaers, J. Oberwinkler, R. Vennekens, T. Gudermann, B.
682 Nilius, and T. Voets. 2011. 'TRPM3 is a nociceptor channel involved in the
683 detection of noxious heat', *Neuron*, 70: 482-94.
- 684 Wagner, T. F., S. Loch, S. Lambert, I. Straub, S. Mannebach, I. Mathar, M. Dufer, A. Lis,
685 V. Flockerzi, S. E. Philipp, and J. Oberwinkler. 2008. 'Transient receptor potential
686 M3 channels are ionotropic steroid receptors in pancreatic beta cells', *Nat Cell*
687 *Biol*, 10: 1421-30.
- 688 Warburg, E. J. 1922. 'Studies on Carbonic Acid Compounds and Hydrogen Ion Activities
689 in Blood and Salt Solutions. A Contribution to the Theory of the Equation of
690 Lawrence J. Henderson and K. A. Hasselbach: Introduction', *Biochem J*, 16: 153-
691 4.
- 692 Yeh, B. I., T. J. Sun, J. Z. Lee, H. H. Chen, and C. L. Huang. 2003. 'Mechanism and
693 molecular determinant for regulation of rabbit transient receptor potential type 5
694 (TRPV5) channel by extracellular pH', *J Biol Chem*, 278: 51044-52.
- 695 Zamudio-Bulcock, P. A., J. Everett, C. Harteneck, and C. F. Valenzuela. 2011.
696 'Activation of steroid-sensitive TRPM3 channels potentiates glutamatergic
697 transmission at cerebellar Purkinje neurons from developing rats', *J Neurochem*,
698 119: 474-85.
- 699 Zhou, Huan-Xiang, and Xiaodong Pang. 2018. 'Electrostatic Interactions in Protein
700 Structure, Folding, Binding, and Condensation', *Chemical reviews*, 118: 1691-
701 741.

702

Figure legends

Figure 1 Inhibitory effect of extracellular acidic pH on TRPM3 activation by PS. (a) Time course of TRPM3 currents elicited by voltage ramps ranging -100 to +100 mV. Both inward and outward currents were completely and reversibly inhibited by pH_o 4.5. 50 μM PS was applied extracellularly and was washed with PS-free extracellular solution between subsequent PS application. Inward and outward currents were measured at -100 and +100 mV, respectively. (b) Representative recording of TRPM3 current in (a) by ramp protocols ranging from -100 to +100 mV at the indicated pH_o . (c) Mean current amplitude of TRPM3 at the indicated pH_o in (a) (mean \pm SEM; $n = 11$, * indicates $p < 0.05$ by unpaired Student's t-test; "n.s." indicates not statistically significant). (d) Current amplitude at the indicated pH_o normalized to the current amplitude at pH_o 7.4 in (a). When compared with pH_o 7.4, p value for pH_o 7.0 and 6.0 were 0.15 and 0.06, respectively. Background electrical activity before application of PS are subtracted in all quantitative analysis. (e) Time course of TRPM3 currents elicited by voltage ramps ranging -100 to +100 mV. PS was applied continuously while reducing extracellular pH without allowing any washing period between subsequent extracellular solution applications. (f) Representative recording of TRPM3 current in (e) by ramp protocols ranging from -100 to +100 mV at the indicated pH_o . (g) Mean current amplitude of TRPM3 at the indicated pH_o in (E) (mean \pm SEM; $n = 7$, * indicates $p < 0.05$ by unpaired Student's t-test; "n.s." indicates not statistically significant). (h) Current amplitude at the indicated pH_o normalized to the current amplitude at pH_o 7.4.

Figure 2 Intracellular acidification blocks TRPM3 activation by PS in a concentration-dependent manner. (a) Representative recordings and time courses (insert) of TRPM3 current by ramp

protocols ranging from -100 to +100 mV at the indicated pH_i. PS was applied through the extracellular solution (pH_o 7.4) and different cells were exposed to different pH_i while keeping that pH_i constant. (b) Mean current amplitude of TRPM3 at the indicated pH_i (mean ± SEM; n = 8 - 14). (c and d) pH_i concentration-dependence of TRPM3 activation by PS. c and d show outward and inward current, respectively, elicited by TRPM3 after extracellular PS application, by voltage ramp ranging -100 to +100 mV. TRPM3 currents exerted at -100 and +100 mV were considered as inward and outward current, respectively, and were utilized for these plots. All currents were normalized to corresponding capacitance of the cell overexpressing hTRPM3-GFP. Each data point is the mean of 8-14 cells with the error bar showing SEM, at the indicated pH_i. Inhibitory pH₅₀ values were measured separately for outward (pH₅₀ = 6.9 ± 0.11) and inward (pH₅₀ = 6.9 ± 0.15) currents.

Figure 3 Concentration–response curve for PS-induced currents in hTRPM3, at the indicated intracellular pH. (a) Time course of TRPM3 currents elicited by voltage ramps ranging -100 to +100 mV. PS was applied extracellularly in increasing concentration sequence at concentrations of 0, 0.1, 1, 10, 20, 50, 100 and 500 μM, with adequate washing period between subsequent PS applications. (b) Representative recording of TRPM3 current at the indicated PS concentration in (a). (c) Mean outward currents measured at +100 mV and normalized to corresponding capacitance of the cell, error bars showing SEM (n = 7 cells), plotted against logarithmic values of PS concentrations. (d) Outward current normalized to maximum concentration-response (500 μM) of the same cell in (c). The EC₅₀ values of PS for the outward currents are 16.4 ± 1.1 μM at pH 7.2 and 15.8 ± 1.1 μM at pH 6.0. (e). Mean inward currents measured at -100 mV and normalized to corresponding capacitance of the cell, error bars showing SEM (n = 7 cells), plotted against

logarithmic values of PS concentrations. (f). Inward current normalized to maximum concentration-response (500 μM) of the same cell in (c). The EC_{50} values of PS for the inward currents are $21.0 \pm 1.0 \mu\text{M}$ at pH 7.2 and $26.0 \pm 1.0 \mu\text{M}$ at pH 6.0.

Figure 4 Inhibitory effect of low intracellular pH on TRPM3 can be reversed by perfusing cells with extracellular solution containing NH_4Cl . (a) Time course showing outward and inward current, recorded at +100 and -100 mV respectively, obtained from HEK cells overexpressing TRPM3, under voltage ramp protocol ranging -100 to +100 mV, ($\text{pH}_i = 6.0$, $n = 11$ cells). Indicated concentrations of NH_4Cl was applied extracellularly along with PS. To achieve similar osmolarity, all extracellular Na^+ concentration was lowered to 85mM and osmolarities were adjusted to 300 ± 10 mOsm by mannitol. Adequate washing time (1 - 3 minutes) was provided after each application of NH_4Cl , to bring the current down to the basal level, which is 6.0 for all the cells recorded. Representative current was plotted versus time in the presence of extracellular NH_4Cl and PS, at the indicated concentrations. To achieve similar osmolarity, all extracellular buffer Na^+ concentration was lowered to 85mM and osmolarities were adjusted to 300 ± 10 mOsm by mannitol. (b) Representative recording of TRPM3 current by ramp protocols ranging from -100 mV to +100 mV at the indicated NH_4Cl concentrations. (c) Mean outward and inward TRPM3 current at the indicated NH_4Cl concentrations (mean \pm SEM, $n=11$ cells). * indicates $p<0.05$ by unpaired Student's t-test. (d) Representative recording of TRPM3 current by the dose-dependent effects of NH_4Cl . The applications of extracellular NH_4Cl at the indicated concentrations. (e) Representative recording of TRPM3 current by ramp protocols ranging from -100 mV to +100 mV at the indicated NH_4Cl concentration. (From panel d) (f) Mean outward and inward TRPM3 current at the indicated NH_4Cl concentration. (From replicated experiment of panel D) (mean \pm SEM,

n=11 cells). (g & h) Concentration-dependence curves of effects of NH₄Cl on TRPM3 activations, outward (g) and inward (h) currents, respectively. All currents were normalized to corresponding capacitance of the cell overexpressing hTRPM3 (mean ± SEM, n=11 cells) at the indicated NH₄Cl concentration. EC₅₀ values were measured separately for outward (NH₄Cl₅₀ = 2.7 ± 0.3 μM) currents, whereas the inward currents continues to increase after applying 60 mM NH₄Cl. (i) Mean ratio of inward current to outward current plotted against NH₄Cl concentrations (mean ± SEM, n=11 cells).

Figure 5 TRPM3 is potentially permeable to protons. (a) Schematic showing the protons permeation recording condition, where all intracellular and extracellular ions were replaced by NMDG and glutamic acid, respectively, except for protons. 50 μM PS was applied while holding hTRPM3-GFP transfected HEK cells at -100 mV. (b) Inward currents were elicited by PS application. No PS activated current under the NMDG solution at pH_o 7.40, while lowering down the pH_o to 5.50 generated a small and transient inward current. Insert panel shows the inward current recorded during NMDG-PS (pH 5.5) application. (c) Mean current amplitude in response to PS at the indicated conditions (mean ± SEM, n = 8 cells). (d) Relative current amplitude in response to PS, comparing with Tyrode (pH_o 7.4) solution response of the same cell (mean ± SEM, n = 8 cells).

Figure 6 Inhibitory effect of intracellular high Ca²⁺ on TRPM3 activation by PS. (a and b) Time course of TRPM3 currents elicited by voltage ramps ranging -100 to +100 mV at the indicated [Ca²⁺]_i concentration. At high [Ca²⁺]_i (1 μM), TRPM3 is activated by PS initially (Black symbol), but runs down soon afterwards (Red symbol). Whereas the TRPM3 current was sustained at the

low $[Ca^{2+}]_i$ condition. Inserts show the representative recordings from the indicated points. (c) Mean current amplitude of TRPM3 at the indicated $[Ca^{2+}]_i$ (mean \pm SEM; n = 10). * indicates $p < 0.05$ by unpaired Student's t-test; "n.s." indicates not statistically significant. (d) Time course and representative recordings of TRPM3 current with $[Ca^{2+}]_i$ (1 μ M) at the indicated pH_i from pH_i 8.0 to pH_i 6.0. (e) pH concentration-dependence of TRPM3 activation by PS at the indicated $[Ca^{2+}]_i$. Green and blue symbols both represent high $[Ca^{2+}]_i$, while green represents currents elicited right after PS application (peak after onset), and blue represent currents remaining after inhibition of by high $[Ca^{2+}]_i$ (80s after onset). All currents were normalized to corresponding capacitance of the cell overexpressing hTRPM3. Each data point is the mean of 8-14 cells with the error bar showing SEM, at the indicated pH_i . (f) Mean ratio of the peak current after onset to the current 80 seconds after onset (mean \pm SEM, n = 8-14 cells). "n.s." indicates not statistically significant among groups by one-way ANOVA with Tukey's post hoc multiple comparison.

Figure 7 Changes of protons sensitivity of TRPM3 mutants. (a) Schematic of TRPM3 structure and the substituted amino acid residues in the putative pore region of hTRPM3. (b) Time course and representative recordings of TRPM3 mutants and wild-type currents elicited by voltage ramps ranging -100 to +100 mV, at the indicated pH_o . Bar graphs show mean outward and inward current amplitudes at the indicated pH_o (mean \pm SEM, n = 7-12 cells) Internal solution had a constant pH of 7.20 for all the recordings. (c) Ratio of outward current amplitudes at pH_o 5.5 and pH_o 7.4, of TRPM3 mutants and WT control. To obtain these ratios, current elicited by +100mV at pH_o 5.5 was divided by the current elicited by +100mV at pH_o 7.4 of the same cell (n = 7-12 cells). P values, comparing each group with WT-TRPM3, * indicates $p < 0.05$ by unpaired Student's t-test; "n.s." indicates not statistically significant.

Supplementary Figure 1 Concentration-dependent effects of NH₄Cl on TRPM3 current. (a) Time course and representative recordings of TRPM3 current by ramp protocols ranging from -100 mV to +100 mV at the indicated NH₄Cl concentrations. The pH_i was 6.0 in all recordings. Individual transfected cells were exposed to NH₄Cl only once. (b) The comparison of effects of NH₄Cl on TRPM3 currents in “gradient” (Fig.4) and “individual” (a) recordings. The increase in outward current in response to NH₄Cl is presented as the percentage increase in outward current from the same cell without NH₄Cl. Both data suggest that NH₄Cl potentiate both TRPM3 inward and outward currents. The average data are mean ± SEM, n = 11-20 cells.

Fig.1

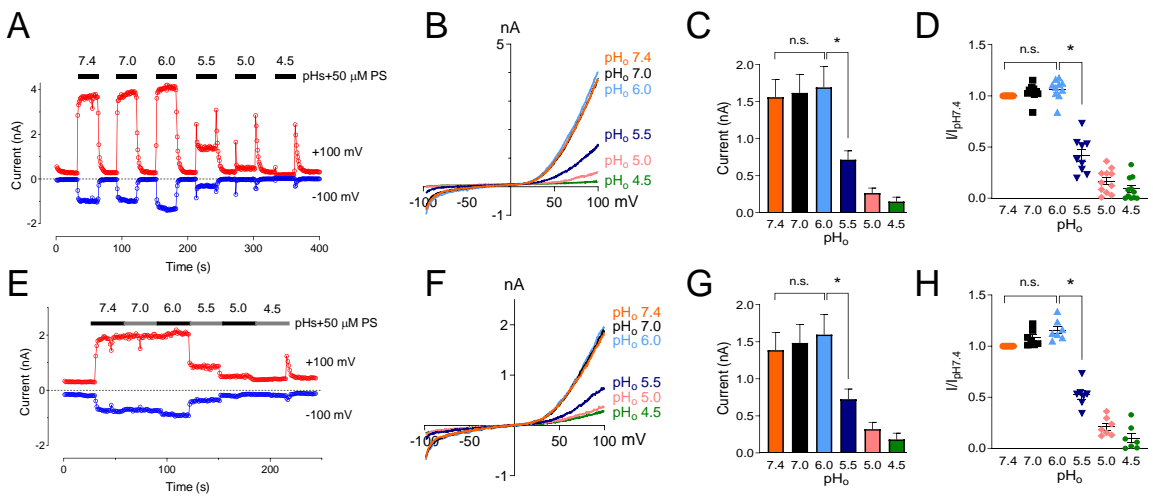


Fig.2

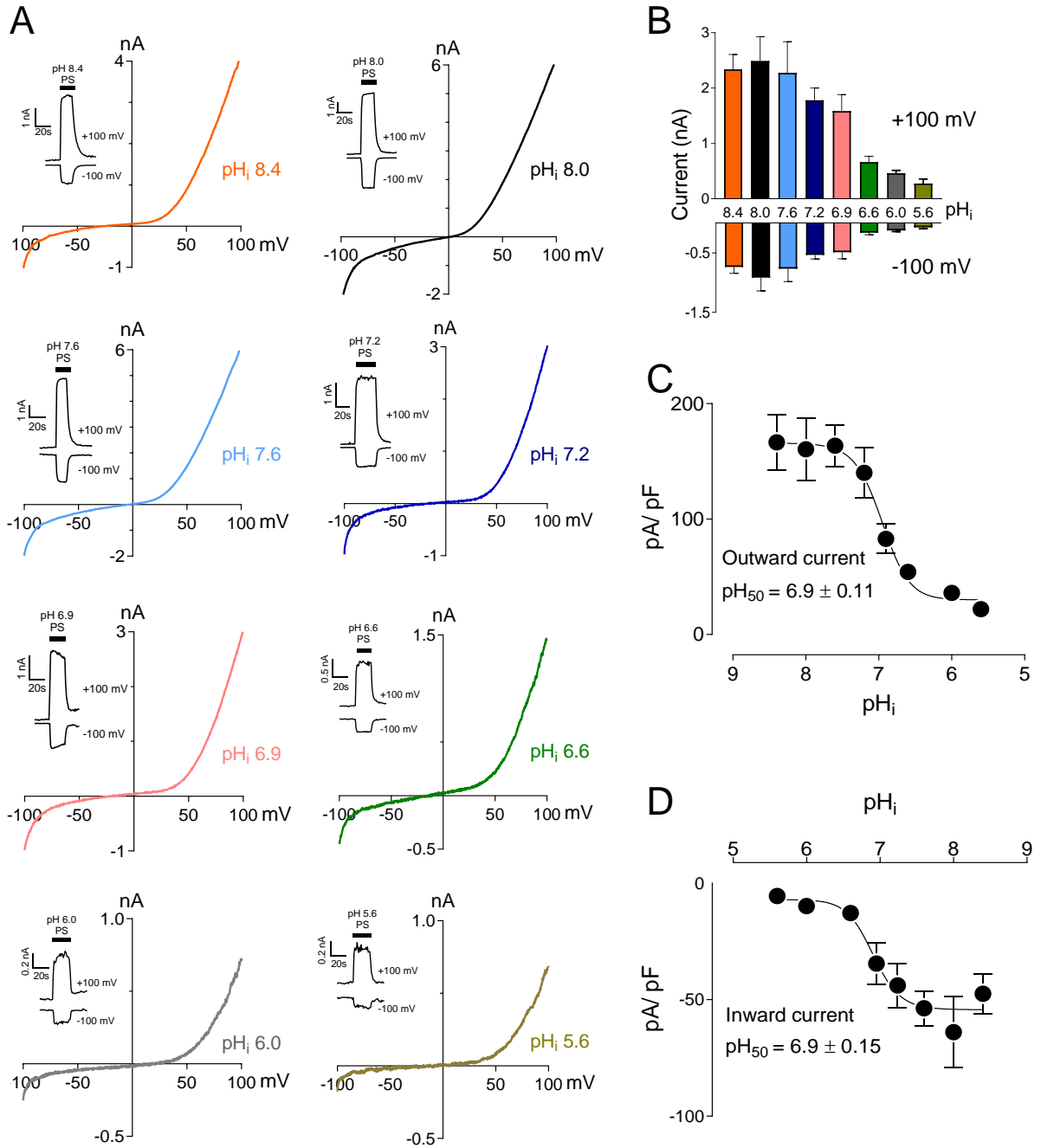


Fig.3

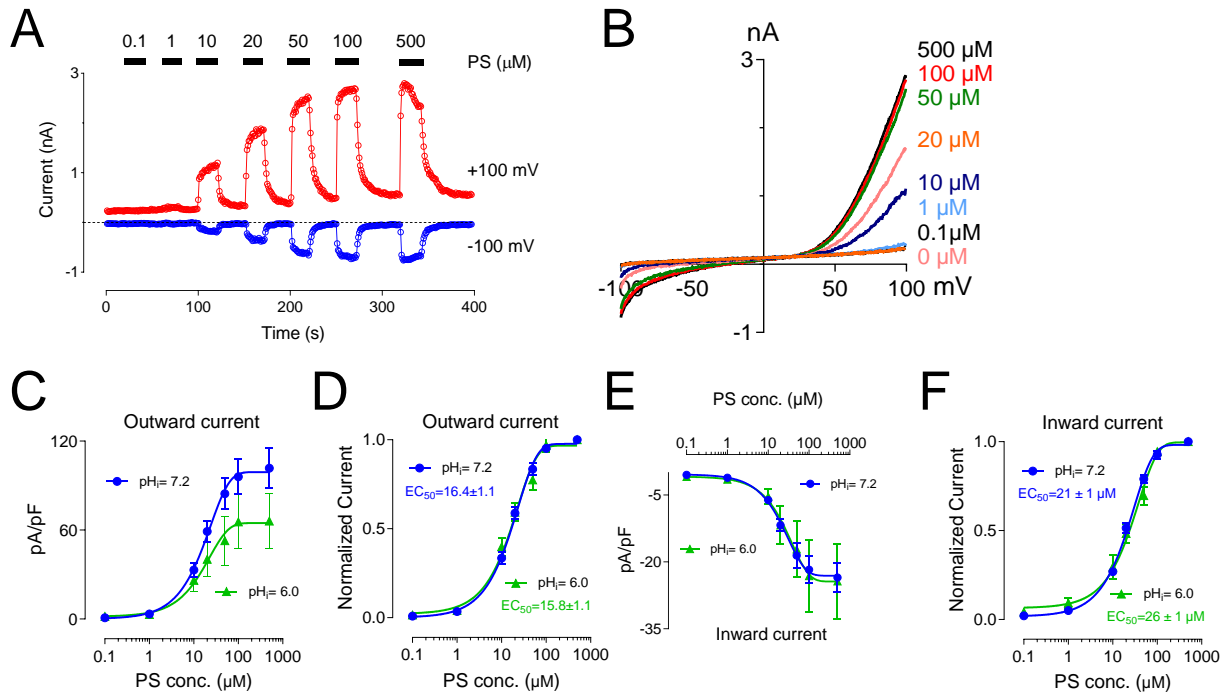


Fig.4

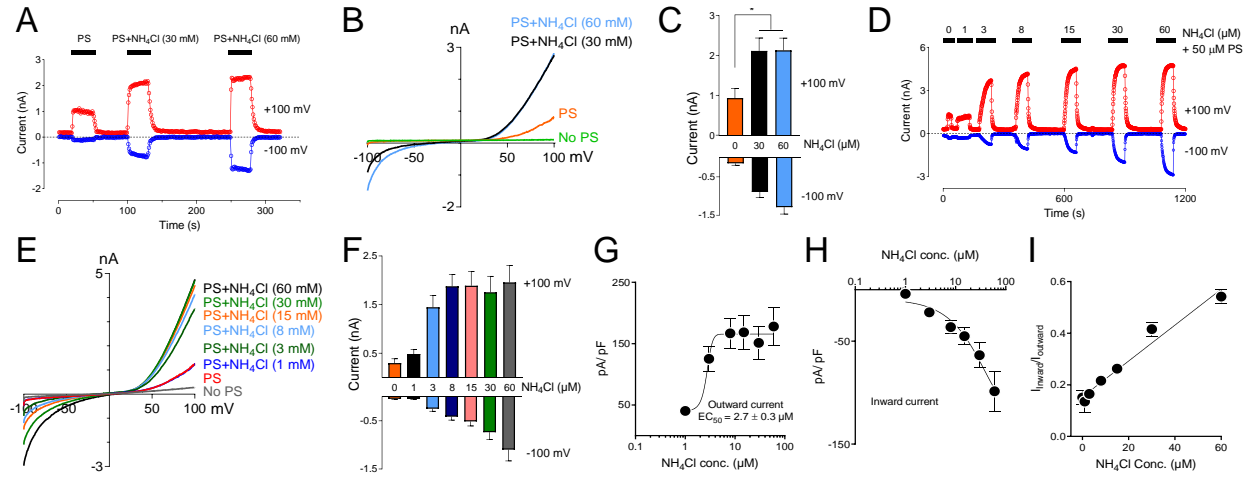


Fig.5

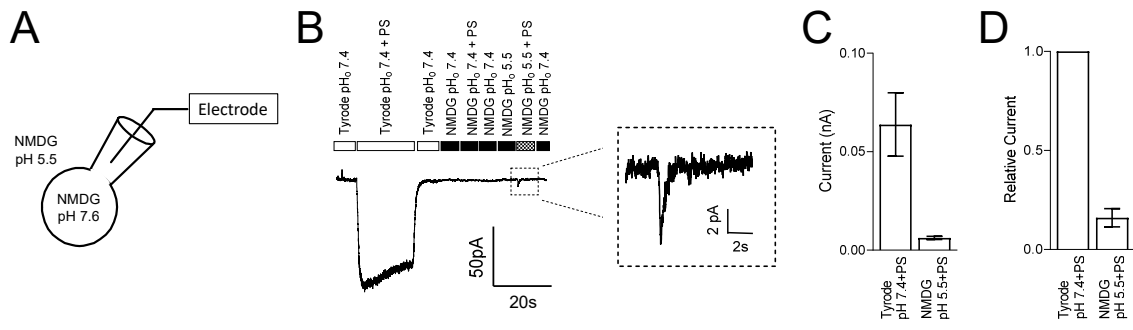


Fig.6

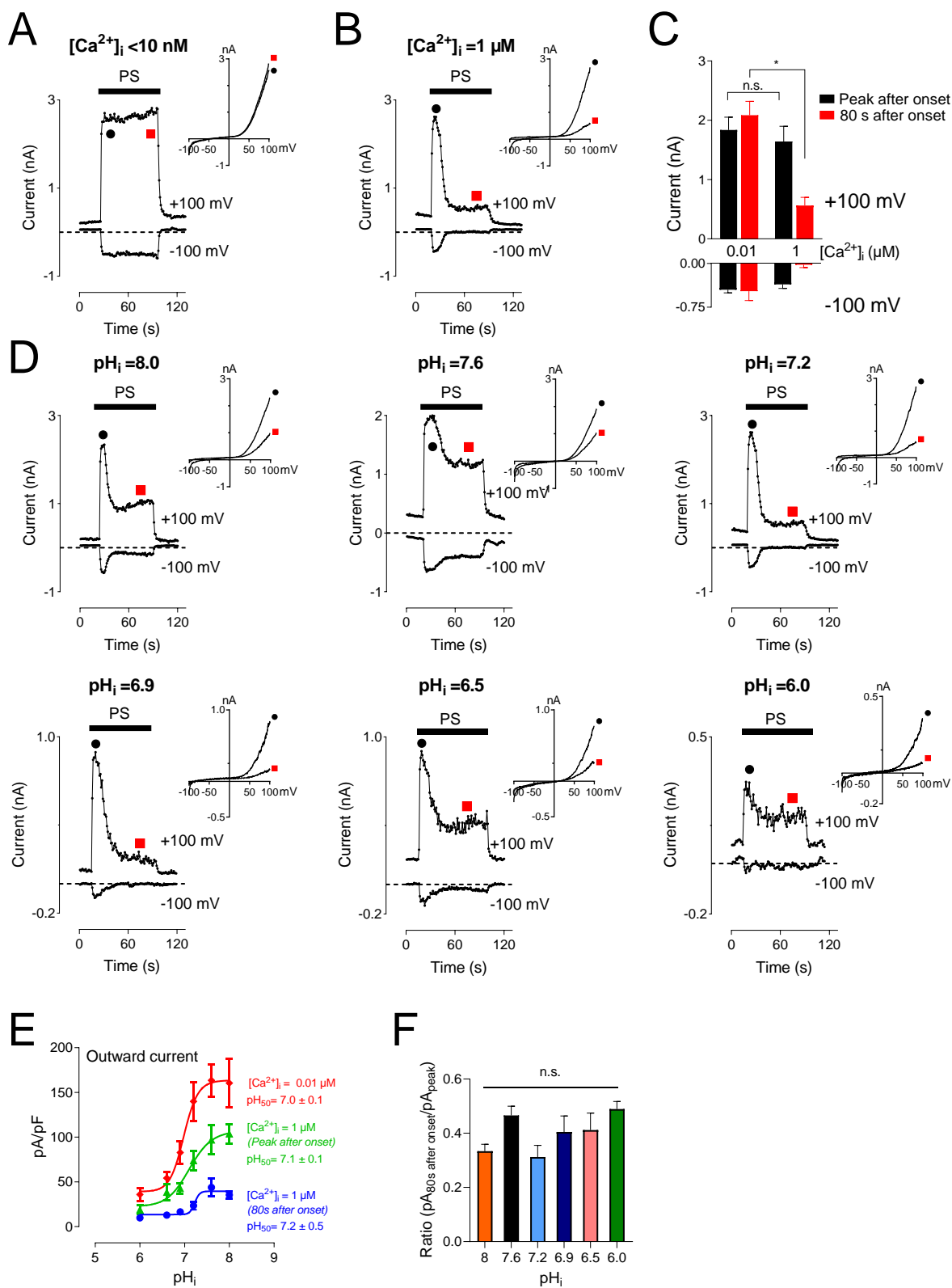
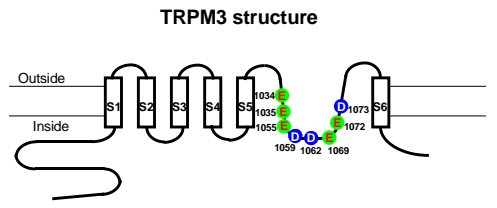
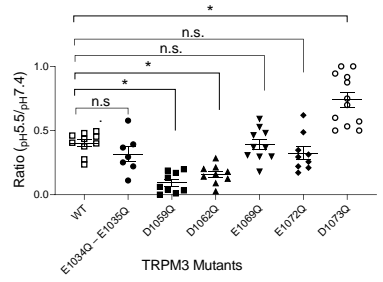


Fig.7

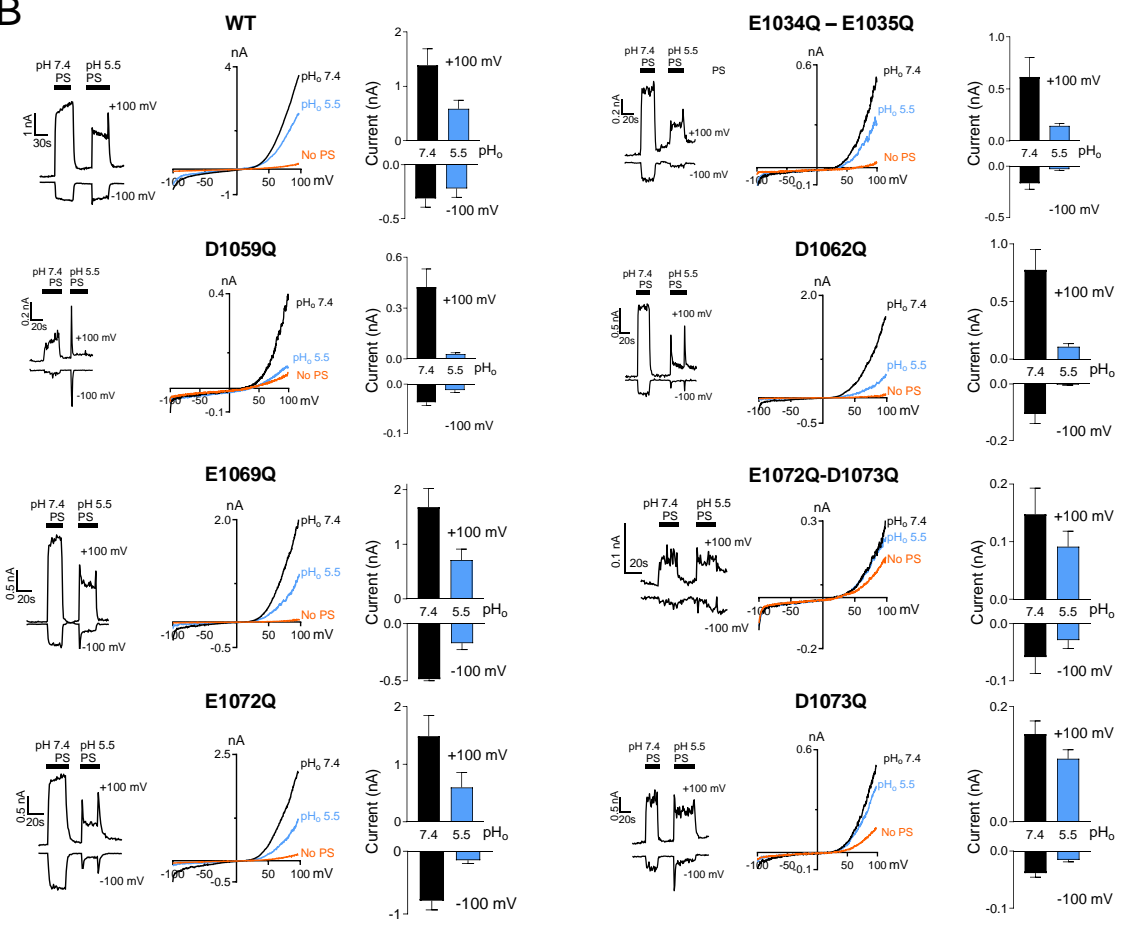
A



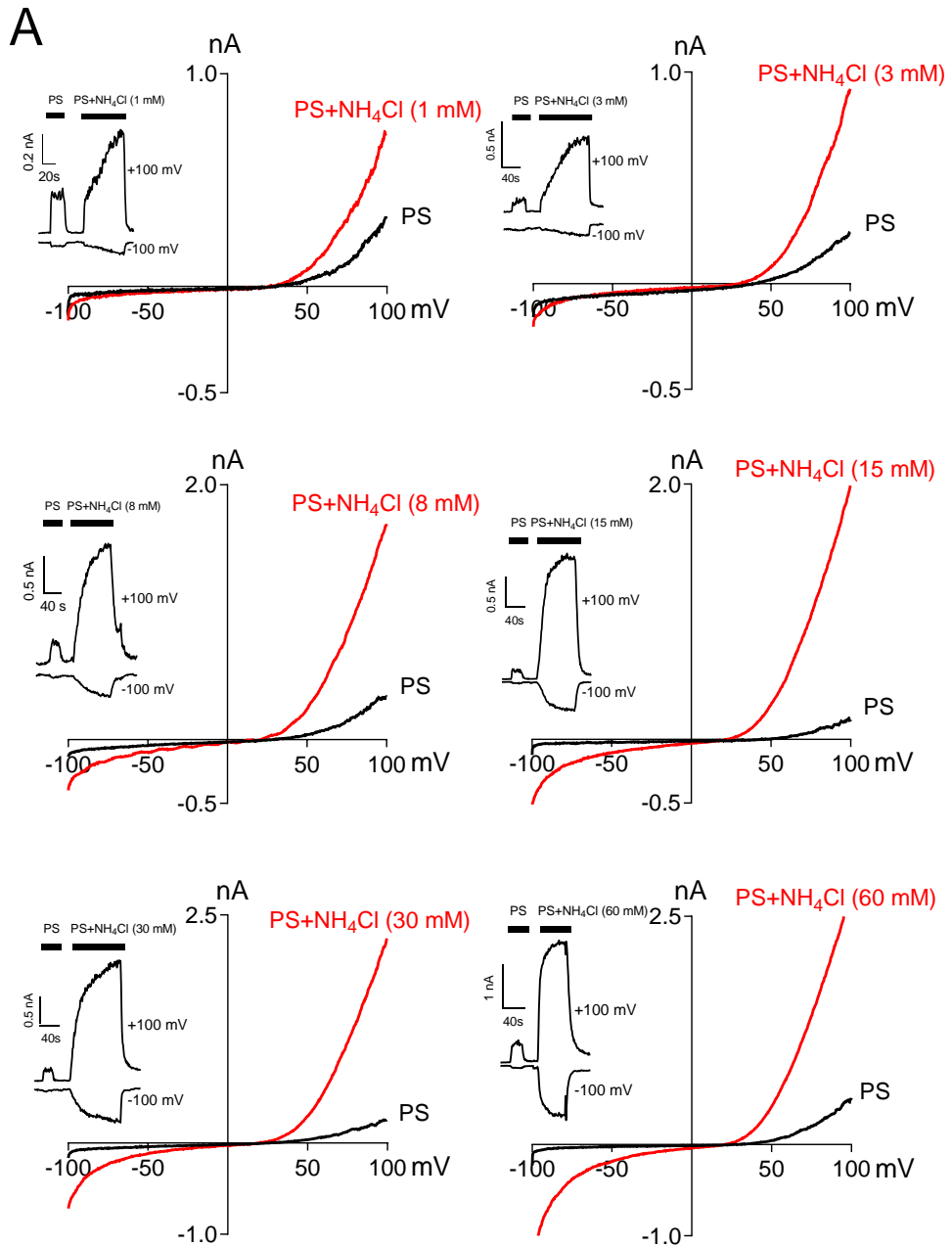
C



B



sFig.1



B

